

Supplemental Material: Reflectance and Shape Estimation for Cartoon Shaded Objects

H. Todo^{†1,2} and Y. Yamaguchi^{1,2}

¹The University of Tokyo, Japan

²JST CREST, Japan

Abstract

This document is the supplemental material for the paper “Reflectance and Shape Estimation for Cartoon Shaded Objects”. In the following, we provide more details on the evaluations of our shading analysis and a few additional examples.

Categories and Subject Descriptors (according to ACM CCS): I.3.3 [Computer Graphics]: Picture/Image Generation—Line and curve generation

I. Comparison of Reflectance Models

Before we start the evaluation of our shading analysis, we compared the visual difference between our target cartoon shading model and a common photorealistic Lambertian model as shown in Figure a. To obtain the ambient reflectance term \mathbf{k}_a and the diffuse reflectance term \mathbf{k}_d for the Lambertian material $\mathbf{c} = \mathbf{k}_a + \mathbf{k}_d I$, we minimize $\|M(I) - (\mathbf{k}_a + \mathbf{k}_d I)\|^2$ with the input color map function M . The color difference suggests that cartoon shading includes some nonlinear parts, which cannot be described by a simple Lambertian model. We will discuss how such a nonlinear reflectance property affects the estimation results.

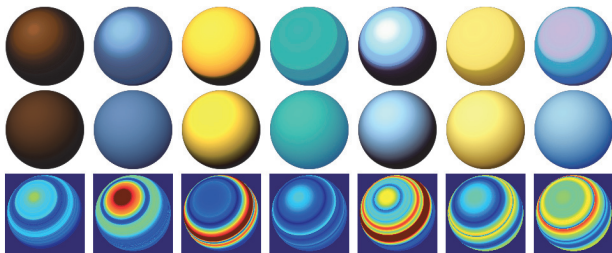


Figure a: Comparison of reflectance models. Top: color map materials selected from our dataset. Middle: Lambertian material fitted to the corresponding color map. Bottom: color difference between the color map materials and Lambertian materials. The materials are listed according to the color difference.

II. Light Estimation

In the early stage of our experiments, we tried to estimate a key light direction \mathbf{L} from the input shading \mathbf{c} and the estimated initial normal \mathbf{N}_0 .

As suggested by [WSTS08], we approximate the problem with a Lambert reflectance $I_c = k_d \mathbf{L} \cdot \mathbf{N}_0$, where the diffuse term $\mathbf{L} \cdot \mathbf{N}_0$ is simply scaled by the diffuse constant k_d . For the input illumination I_c , we compute the luminance value from the original color \mathbf{c} as the L component in Lab color space. We estimate the light vector \mathbf{L} by minimizing the following energy:

$$E_L(\mathbf{L}') = \sum_{\Omega} \|I_c - \mathbf{L}' \cdot \mathbf{N}_0\|^2, \quad (1)$$

where \mathbf{L}' is resulted as $\mathbf{L}' = k_d \mathbf{L}$. We finally obtain the unit light vector $\mathbf{L} = \frac{\mathbf{L}'}{\|\mathbf{L}'\|}$ to normalize \mathbf{L}' . The diffuse reflectance constant k_d is optionally computed from $k_d = \|\mathbf{L}'\|$.

Figure b summarizes our experiment for light estimation. In this experiment, we give a single ground-truth light direction \mathbf{L}_t (top left) to generate the input cartoon shaded image \mathbf{c}_t and then estimate a key light direction \mathbf{L} by solving Equation 1.

It can be observed that the estimated results look consistent with near-Lambertian materials (the left 3 maps) but inconsistent with more stylized materials (the right 3 maps). Another important factor is the shape complexity. The estimated light direction is relatively consistent with rounded smooth shapes. However, the light estimation error becomes quite large when the input model contains many crease edges especially around the silhouette.

The result suggests us that we require additional constraints to improve the light estimation quality. In the following experiments,

[†] Present affiliation: Tokyo University of Technology, Japan

we simply provide a ground-truth light direction \mathbf{L}_t to quantitatively measure the error of each analysis step.

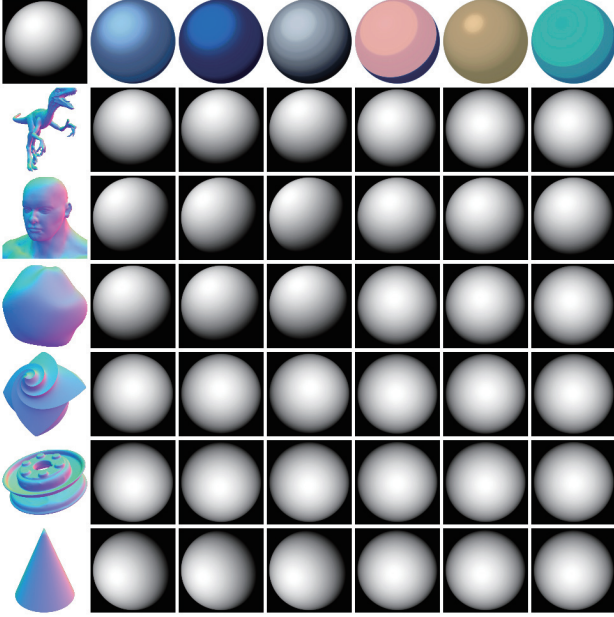


Figure b: Light estimation error. Top left: the input ground-truth light direction \mathbf{L}_t . Top row: the input color map materials shaded from the \mathbf{L}_t . The left 3 maps from the small average errors. The right 3 maps from the large average errors. Left column: the input 3D models. The top 3 models from the small average errors. The bottom 3 models from the large average errors.

III. Shading Analysis

In this section we provide additional details describing the evaluations of our shading analysis. Figure c illustrates our estimation results with different color map materials. Although our method distributes certain shading errors near the boundaries of the color areas, it recovers a relatively smooth normal field and shading appearance similar to ground-truth.

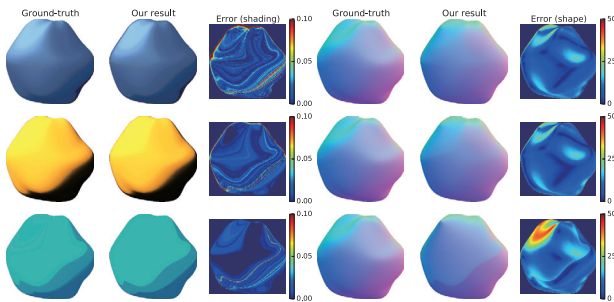


Figure c: Shading analysis results from different color map materials.

We also compute the mean squared error (MSE) to quantitatively

compare estimated results (see Figure d, e, f and g). We cannot observe the significant difference from the MSE comparisons Figure d and e to support the effectiveness of our method against the shape difference. In both comparisons, our method tends to distribute less errors for simple rounded shapes but the errors become larger than the Lambert assumption for more complex shapes.

Figure f shows that our method recovered better illumination results except one near Lambertian material. However, the color difference from the Lambertian material cannot describe these illumination errors and the shape errors in Figure g. We require a more valid measurement to distinguish these material differences.

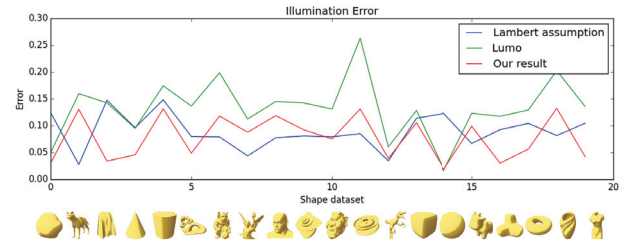


Figure d: Errors of estimated illumination depending on the input shape. Our method tends to distribute less errors for simple rounded shapes.

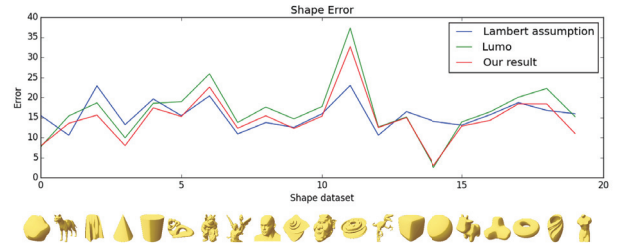


Figure e: Errors of estimated shape depending on the input shape. Overall results are similar to the illumination error but the errors become larger depending on the shape complexities.

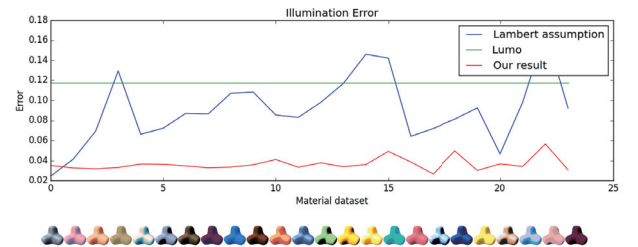


Figure f: Errors of estimated illumination depending on the input material (sorted by the color distance from the corresponded Lambertian materials). Except one near Lambertian material, our method recovered the best illumination results.

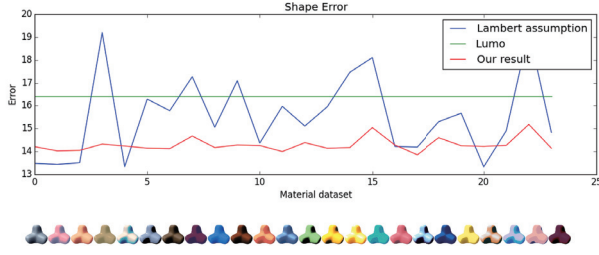


Figure g: Errors of estimated shape depending on the input material. Compared to the illumination error, the estimated result is unrelated to the material difference.

IV. Real Illustration Examples

We have tested our shading analysis approach for three different shading styles on real illustrations. The material regions are relatively simple, but each material region is painted with different quantization effects.

To apply our shading analysis and relighting methods, we first manually segmented material regions for the target illustration. We also provide a key light direction for the target illustration, which is used in our reflectance estimation step.

Compared to the ideal cartoon shading in our evaluations, a material region in the real examples may include non-diffuse parts. As suggested by a photorealistic illumination estimation [KSES14], we encode such specular and shadow effects as residual difference $\Delta \mathbf{c} = \mathbf{c} - M(\mathbf{L} \cdot \mathbf{N})$ from our assumed shading representation $\mathbf{c} = M(\mathbf{L} \cdot \mathbf{N})$.

As shown in Figure i and the supplemental videos, the residual representation can recover the appearance of the original shading. We also note that our initial experiment produced possible shading transitions for diffuse while specular and shadow effects are relatively static.

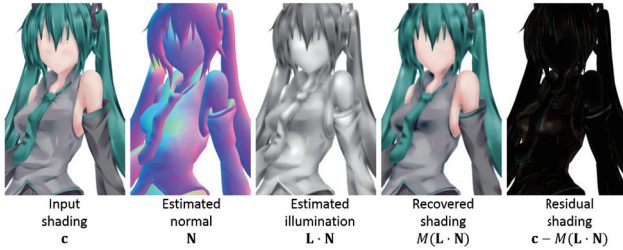


Figure h: Reflectance and shape estimation result for the real illustration example. Non-diffuse parts are encoded as residual shading.

V. Limitations

The fundamental limitation of our current formulation is that we only minimize the appearance error $\|\mathbf{c} - M(\mathbf{L} \cdot \mathbf{N})\|^2$. While we can closely recover the original input shading appearance, the estimated shapes can result in large errors.



Figure i: Relighting sequence with our method. Non-diffuse parts are limited to static transitions with the simple residual representation.

As shown in Figure j, our method cannot recover the input shape even if the material is Lambertian reflectance with full illumination constraints. In particular, shape estimation errors tend to become large for complicated shapes such as Pulley or Lucy.

Even for practical scenarios, shape estimation is important to significantly affect the relighting results. We are currently investigating how to incorporate interior contour constraints [Joh02] and more flexible user constraints [OZM*06, WSTS08, SBSS12] for initial normal estimation.

Another type of limitation is related to the assumed shading model. Our relighting scheme lacks specular and shadow effects, which will be treated as the residual effects. For more practical situations, incorporating such specular and shadow models is an important future work. While large collections of 2D digital illustrations are available from online sources, we cannot directly apply our method since we require manual segmentation tasks. A crucial area of future research is to automate albedo estimation, as suggested by intrinsic images [GJAF09, RKZ*11].

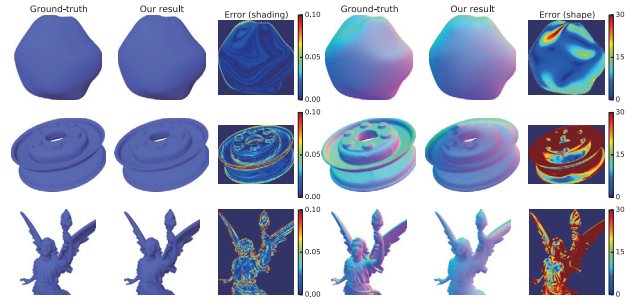


Figure j: Shape analysis result in the case of Lambertian reflectance. Blob (top): selected from small errors in shape and shading. Pulley (middle): selected from large errors in shape. Lucy (bottom): selected from large errors in shading.

References

- [GJAF09] GROSSE R., JOHNSON M. K., ADELSON E. H., FREEMAN W. T.: Ground truth dataset and baseline evaluations for intrinsic image algorithms. In *IEEE 12th International Conference on Computer Vision* (2009), IEEE, pp. 2335–2342. 3
- [Joh02] JOHNSTON S. F.: Lumo: Illumination for cel animation. In *Proceedings of NPAR 2002* (New York, NY, USA, 2002), ACM, pp. 45–52. 3

- [KSES14] KHOLGADE N., SIMON T., EFROS A., SHEIKH Y.: 3d object manipulation in a single photograph using stock 3d models. *ACM Trans. Graphics (SIGGRAPH 2014)* 33, 4 (July 2014), 127:1–127:12. [3](#)
- [OZM*06] OKABE M., ZENG G., MATSUSHITA Y., IGARASHI T., QUAN L., YEUNG SHUM H.: Single-view relighting with normal map painting. In *Proceedings of Pacific Graphics 2006* (2006), pp. 27–34. [3](#)
- [RKZ*11] ROTHER C., KIEFEL M., ZHANG L., SCHÖLKOPF B., GEHLER P. V.: Recovering intrinsic images with a global sparsity prior on reflectance. In *Advances in Neural Information Processing Systems* 24 (2011), pp. 765–773. [3](#)
- [SBSS12] SHAO C., BOUSSEAU A., SHEFFER A., SINGH K.: Crossshade: Shading concept sketches using cross-section curves. *ACM Trans. Graphics (SIGGRAPH 2012)* 31, 4 (July 2012), 45:1–45:11. [3](#)
- [WSTS08] WU T.-P., SUN J., TANG C.-K., SHUM H.-Y.: Interactive normal reconstruction from a single image. *ACM Transactions on Graphics (SIGGRAPH Asia 2008)* 27, 5 (Dec. 2008), 119:1–119:9. [1](#), [3](#)